

## ESTIMATION OF TOTAL HETEROGENEITY PROPERTIES OF CARBON NANOTUBES

D. Sternik<sup>1</sup>, M. Błachnio<sup>1</sup>, P. Staszczuk<sup>1\*</sup>, G. W. Chądzyński<sup>2</sup> and E. Kowalska<sup>3</sup>

<sup>1</sup>Department of Physicochemistry of Solid Surface, Chemistry Faculty, Maria Curie-Skłodowska University  
Maria Curie-Skłodowska Sq. 3, 20-031 Lublin, Poland

<sup>2</sup>Technical University, Wybrzeże Wyspiańskiego Str. 27, 50-370 Wrocław, Poland

<sup>3</sup>Industrial Institute of Electronics, Długa Str. 44/50, 00-241 Warsaw, Poland

Physico-chemical properties (adsorption capacity, desorption energy distribution and pore-size distribution functions) of nanomaterial surfaces from selected materials, based on sorptometric and liquid thermodesorption measurements under quasi-equilibrium conditions, are presented. The fractal dimensions of nanotubes using sorptometric and AFM data have been evaluated.

Comparison of thermogravimetric and other data provide new information about the adsorption and pore structure of the studied materials. The fractal dimensions of nanomaterial surfaces using sorptometry are in good agreement with those from AFM.

**Keywords:** AFM methods, desorption energy, nanotubes, sorptometry, thermogravimetry Q-TG, total heterogeneity

### Introduction

Carbon nanotubes are a new allotropic form of carbon and possess interesting physico-chemical properties. The adsorption and porosity properties of carbon nanotubes are not widely presented in literature. Their chance discovery was a result of an enormous interest in fullerenes. Carbon nanotubes are built of graphene layers and can assume single- or multi-wallet structures [1, 2].

The study of nanotubes is an important aspect of the science of nanotechnology. It is one of the most dynamically developing field of science and technology, based on solid state physics, materials technology, molecular biology and chemistry [3, 4]. It involves the production of materials and structures not exceeding 100 nm dimensions. It has applications in the construction of more effective computers, drug synthesis and accurate measurements [5]. Chemical modifications of nanotubes in both open terminated areas and on outer and inner walls create many possibilities. However, this field of science is still in the position of theoretical predictions and few projects are accomplished in practice.

Prospective and present applications of nanotubes depend on their physico-chemical properties. Compared with other materials, they have desirable properties for many applications. The most important of these are density, resistance to stretching and bending, thermal and electrical conductivity, field emission and resistance to temperature. Good adsorption properties of nanocarbon materials contribute to their

extensive practical applications. This paper aims to estimate adsorption and porosity properties of double- and multi-wallet carbon nanotubes.

### Experimental

#### Materials and apparatus

Five carbon nanomaterial samples produced by the Sigma-Aldrich Co. were investigated (O.D. – outer diameter, I.D. – inner diameter and  $l$  – length of nanotubes):

- A1 – multi-wallet carbon nanotubes; O.D.=3–10 nm, I.D.=1–3 nm,  $l$ =0.1–10  $\mu$ m;
- A2 – multi-wallet carbon nanotubes; O.D.=10–20 nm, I.D.=5–10 nm,  $l$ =0.5–200  $\mu$ m;
- A3 – multi-wallet carbon nanotubes; O.D.=20–40 nm, I.D.=5–10 nm,  $l$ =0.5–200  $\mu$ m;
- A4 – multi-wallet carbon nanotubes; O.D.=60–100 nm, I.D.=5–10 nm,  $l$ =0.5–500  $\mu$ m;
- A5 – double-wallet carbon nanotubes; diam.=1.3–5 nm,  $l$ =50  $\mu$ m.

Thickness of the adsorbed liquid layers on the surface can be assessed by means of immersion of the solid samples. Adsorption of non-polar (benzene and *n*-octane) and polar (water and *n*-butanol) liquid layers was measured using a derivatograph Q-1500 D (MOM, Hungary). The samples were saturated with liquid vapours in a vacuum desiccator at  $p/p_0=1$ . The Q-TG mass loss and Q-DTG differential mass loss

\* Author for correspondence: piotr@hermes.umcs.lublin.pl

curves were measured under quasi-isothermal conditions in the temperature range 20–250°C at a heating rate of 6°C min<sup>-1</sup>.

Porosity properties, e.g. specific surface area, pore size distribution and pore volume, were calculated from low temperature nitrogen adsorption–desorption isotherms measured by means of a Sorptomat ASAP 2405 V1.01 (Micrometrics Co., USA). In order to characterize fully the structure of nanomaterial surfaces, AFM images were also obtained by means of a Digital Instruments (USA) NanoScope III type.

## Results and discussion

Studies of the structure of materials with nanometric dimensions require precise measuring tools and techniques. For the carbon nanotubes presented in this paper, three independent techniques were used, namely, sorptometry, Q-TG liquid thermodesorption under quasi-static conditions and atomic force microscopy (AFM).

### Measurements of nitrogen sorption

Figure 1 presents nitrogen sorption isotherms at 77 K for the A4 and A5 samples. They are of type II according to the IUPAC classification. This type of isotherm describes the process of physical adsorption of nitrogen on the adsorbent surface. Because carbon nanotubes have a heterogeneous porous structure, micropores with the smallest diameters are filled up at low pressures of the adsorbate. With increasing adsorbate gas pressure, pores of larger diameter are filled up and the multi-layer adsorption takes place. The presence of the hysteresis loop in the sorption

isotherms is evidence for occurrence of open capillaries in the adsorbents. During adsorption a liquid surface of cylindrical shape is formed in the capillaries until they are completely filled up. However, in the desorption process two layers of adsorbate molecules are formed in the shape of spherical cone. As a result, the adsorption curve does not overlap with the desorption curve in the capillary condensation area. The adsorption capacities read from the isotherms are characterized by large values (Table 1). The A5 double-wallet nanotubes have the largest adsorption capacity i.e. 1350 cm<sup>3</sup> g<sup>-1</sup>. For the other nanomaterials the values are in the range 440–920 cm<sup>3</sup> g<sup>-1</sup>.

To obtain detailed information about the texture of the studied nanomaterials, the following parameters were determined: adsorption capacity, specific surface area, pore volume, pore size and pore-size distribution functions (Fig. 2). The mean pore radius and the pore volume of samples were calculated from the desorption isotherms using the Barrett–Joyner–Halenda (BJH) method and the specific surface areas from the Brunauer–Emmett–Teller (BET), Langmuir and BJH theories and methods.

The specific surface area ( $S_{\text{BET}}$ ) vary in the range 178.6–294 cm<sup>2</sup> g<sup>-1</sup> for the samples of multi-wallet nanotubes and are in the order, A3<A1<A4<A2. These changes are due to the sizes of elementary cells and length of nanotubes. The specific surface area of the double-wallet nanotubes A5 has the highest value,  $S_{\text{BET}}=742.85$  cm<sup>2</sup> g<sup>-1</sup>, of all studied nanomaterials.

For the A4 sample the decrease of the mean value of pore radius with the increasing specific area and volume of micropores is observed. The sample A2 is without micropores and possesses the largest mean pore radius. In all the materials studied, pores of radii close to 10 nm make the largest contribution to sorption.

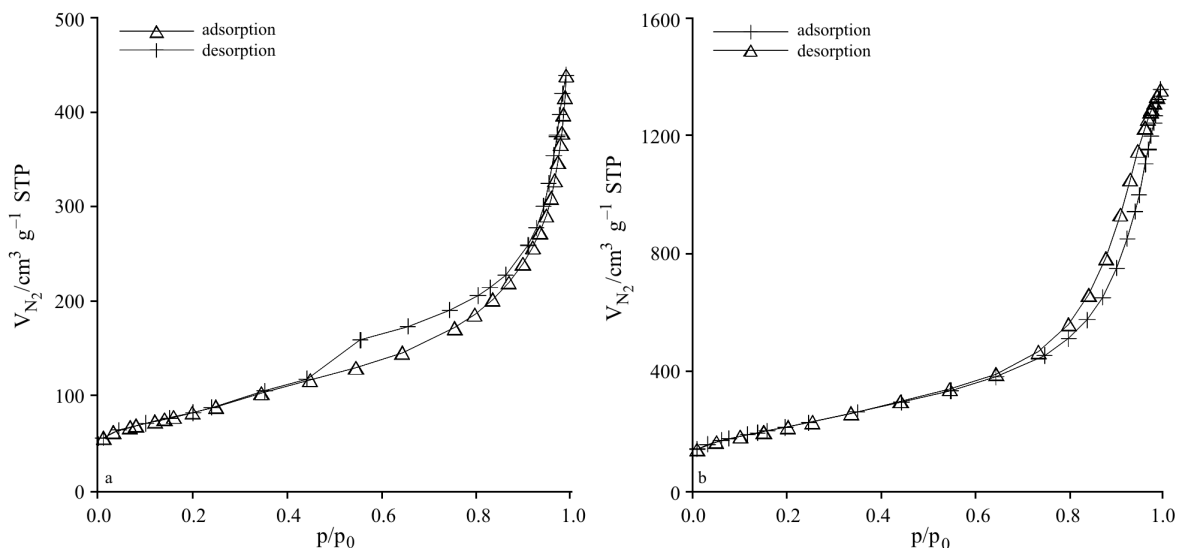
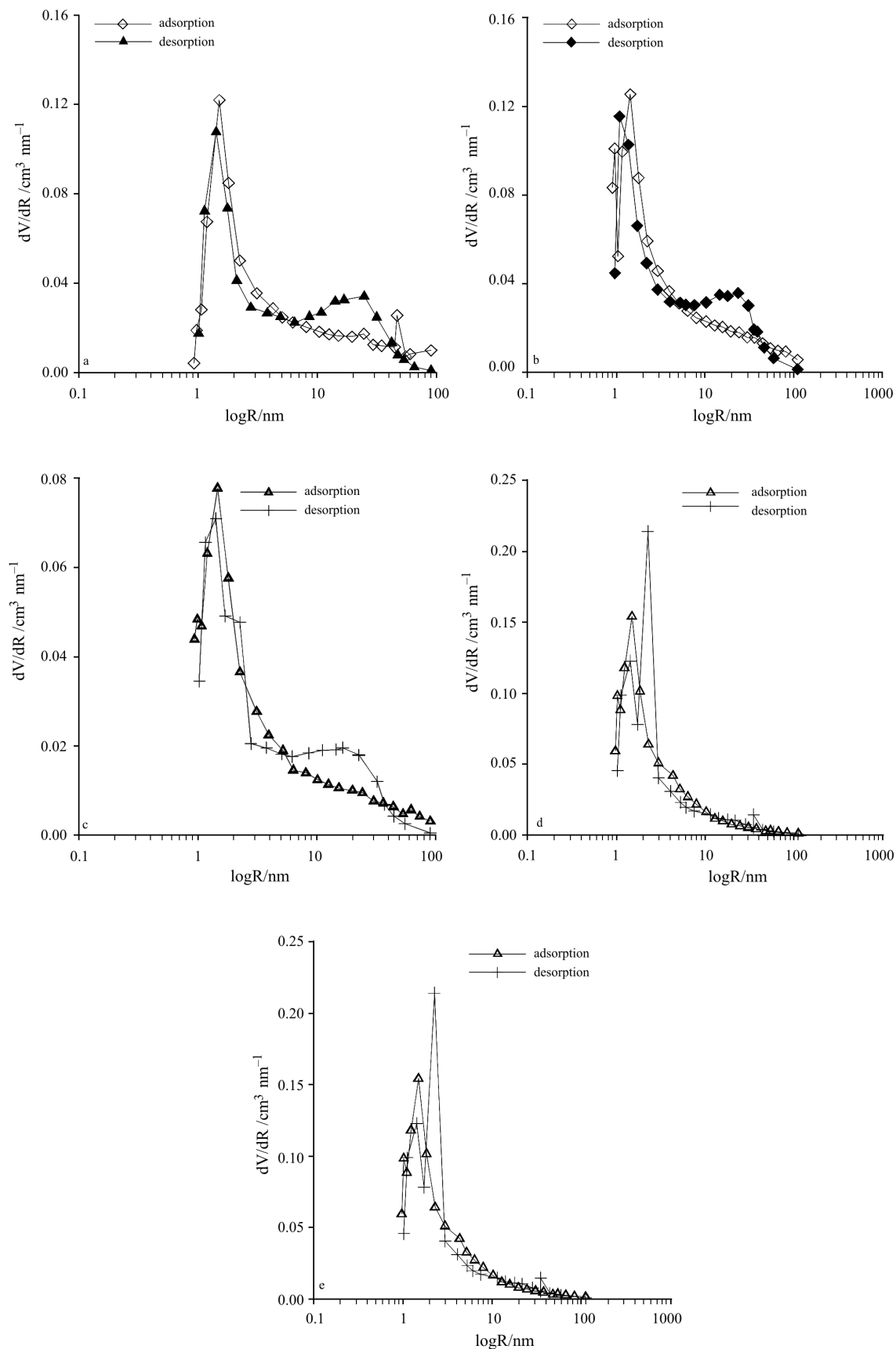


Fig. 1 Nitrogen adsorption and desorption isotherms for a – A4 and b – A5 samples



**Fig. 2** Distribution functions of pore volume in relation to their radius for the studied samples; a – A1, b – A2, c – A3, d – A4 and e – A5 sample

**Table 1** Adsorption and structural parameters of carbon nanotubes

Sample	$a_{\max}/\text{cm}^3 \text{ g}^{-1}$	$S_{\text{BET}}/\text{m}^2 \text{ g}^{-1}$	$V_{\text{BJH ads}}/\text{cm}^3 \text{ g}^{-1}$	$V_{\text{BJH des}}/\text{cm}^3 \text{ g}^{-1}$	$D_{\text{BJH av}}/\text{nm}$	$D_{\text{BET av}}/\text{nm}$
A1	780	244.32	1.22	1.22	17.65	13.67
A2	920	294.10	1.43	1.42	16.95	13.96
A3	440	178.59	0.69	0.68	14.01	12.07
A4	440	289.17	0.69	0.69	8.81	8.08
A5	1350	742.85	2.13	2.10	10.19	10.57

Figure 2 presents the pore-size distribution functions  $dV/dR=f(R)$ , where  $V$  is the pore volume and  $R$  the pore radius. As can be seen, the maxima occur in the pore radius range 2–4 nm. The concentration of micro- and mesopores decreases with increasing pore radius. The observed shapes of the pore-size distribution curves are bimodal for the A1, A2 and A3 samples and Gaussian for A4 and A5 samples.

Studies of carbon nanostructures showed the relation between porosity and number of graphene layers. The carbon nanotube consists of one or a few graphene layers combined into a spatial structure by mean of Van der Waals interactions. The gaps between the individual graphene layers with the core interiors form micropores. However, free spaces in the nanotube clusters of chaotic or ordered arrangement towards each other form a well-developed mesoporous structure. In the case of double-wallet nanotubes (e.g. A5 sample) a significant increase of pore volume towards multi-wallet materials is observed. The pore distribution functions in relation to their radii show that the studied materials can be included into mesoporous adsorbents with the additional presence of micropores. The exception is sample A2, in which the contribution of micropores on the surface is not observed.

Carbon nanotubes are characterized by self-resemblance; this means that they can be segmented into parts, which are geometrically similar to the whole. In other words, they are fractal objects. Thus fractal coefficients were used for structural estimation of nanotube materials. They were calculated from the isotherms of low-temperature nitrogen adsorption and desorption by the methods based on the Frenkel,

Halsey and Hill as well as Kiselev theory [6]. To compare the obtained values, additionally the fractal coefficients were determined by the independent method using the AFM data from The Scanning Probe Image Processor program [7, 8]. The results are given in Table 2. The mean values of volumetric fractal coefficients from the sorptometric measurements vary in the range 2.57–2.61 which indicates heterogeneous distribution of pores. With increasing  $D_f$  values, relative contribution of the pores of the values close to the maximum increases. These data correlate well with the surface fractal coefficients calculated on the basis of Fourier transformation from the AFM images.

#### Thermogravimetric studies

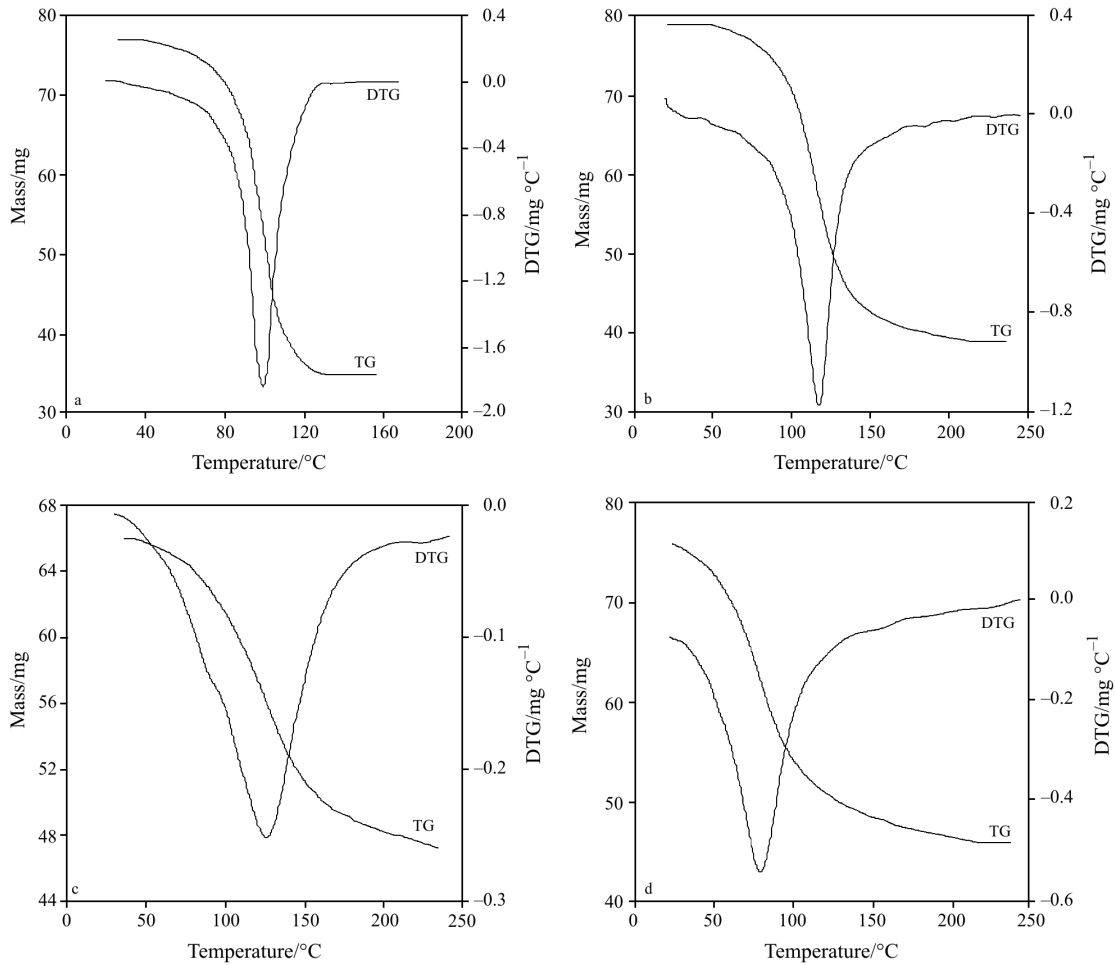
The thermodesorption method under quasi-isothermal conditions used to study properties of the liquid/carbon nanomaterials systems is characterized by wide range of applications, high selectivity and resolution.

Figure 3 presents curves for liquid thermodesorption from the surface of the studied samples. The Q-DTG curves describe the energetic state of liquid molecules on the surface of carbon nanotubes. The energy of interactions between molecules depends on the nature of adsorbate, properties of the surface on which they are adsorbed and porosity of the sample (presence of meso- and micro-pores). The differential Q-DTG curves are characterized by the presence of one distinct peak. This is evidence for continuity of thermo-desorption and monotonic change of adsorption layer properties depending on the distance from the liquid molecule surface; these molecules are bound to the surface by the forces of different magnitude and range. In subsequent stages of sample desorption, adsorbed liquid layers (range of capillary condensation) remaining within the range of surface forces, and active surface centres are removed. Liquid adsorption with active centres on the surface depends on bonds of the same type.

The method of programmed liquid thermodesorption from the surface of studied solids can be used for calculation of desorption energy and presentation of the desorption energy distribution function in a graphical form (Fig. 4).

**Table 2** Values of volumetric fractal coefficients calculated using two methods based on the nitrogen adsorption isotherms and the surface fractal coefficients determined by means of AFM method

Sample	Sorptometric measurements, $D_{f \text{ av}}$	AFM, $D_f$
A1	2.61	2.56
A2	2.57	2.46
A3	2.59	2.57
A4	2.58	2.58
A5	2.59	2.51



**Fig. 3** Q-TG and Q-DTG curves of thermodesorption of liquids from the surface of the sample A5 under the quasi-static conditions; a – water/A5, b – *n*-butanol/A5, c – *n*-octane/A5 and d – benzene/A5

Monomolecular desorption kinetics, in the case of unassociated one-component layers, is described by the equation:

$$-\frac{d\theta}{dt} = v(1-\theta)\exp\left(-\frac{E_d}{RT}\right) \quad (1)$$

where

$$T = T_0 + \beta t \quad (2)$$

and  $R$  – universal gas constant;  $\theta$  – the degree of surface coverage;  $v$  – entropy factor;  $E_d$  – desorption energy calculated for each temperature;  $T_0$  and  $T$  – initial and given temperatures of desorption, respectively;  $\beta$  – the heating rate of the sample and  $t$  – time.

Equation (1) holds for the case when the amount of desorbed substance does not fill the whole surface uniformly; however, desorption takes place in the range of capillary condensation. The above equation can be also used for the analysis of desorption from the multilayer filled energetically on the heterogeneous surface of the studied material. Then the desorption rate is described by the integral equation:

$$-\frac{d\theta}{dT} = \int_{E_d} \varphi(E_d)(1-\theta)\frac{v}{\beta}\exp\left(-\frac{E_d}{RT}\right)dE_d \quad (3)$$

Energetic heterogeneity of the solid surface is described by the energy distribution function  $\varphi(E_d)$ . In other words, this is density of adsorption centre distribution probability on the surface of the studied sample in relation to the quantity of desorption energy [9, 10].

The logarithmic form of the initial equation is expressed by the following formula [11]:

$$\ln\left(-\frac{1}{1-\theta}\frac{d\theta}{dT}\right) = f\left(\frac{1}{T}\right) \quad (4)$$

The final expression to determine the density function  $\varphi(E_d)$  can be presented as:

$$\varphi(E_d) = -\frac{d\theta}{dT} \frac{1}{T} \quad (5)$$

Tables 3 and 4 present the ranges of  $E_d$  and  $Q_{E_d, \max}$  changes for individual systems. The shape of curves of desorption energy distribution functions presented in Fig. 4 are similar to the Gaussian curves with one dis-

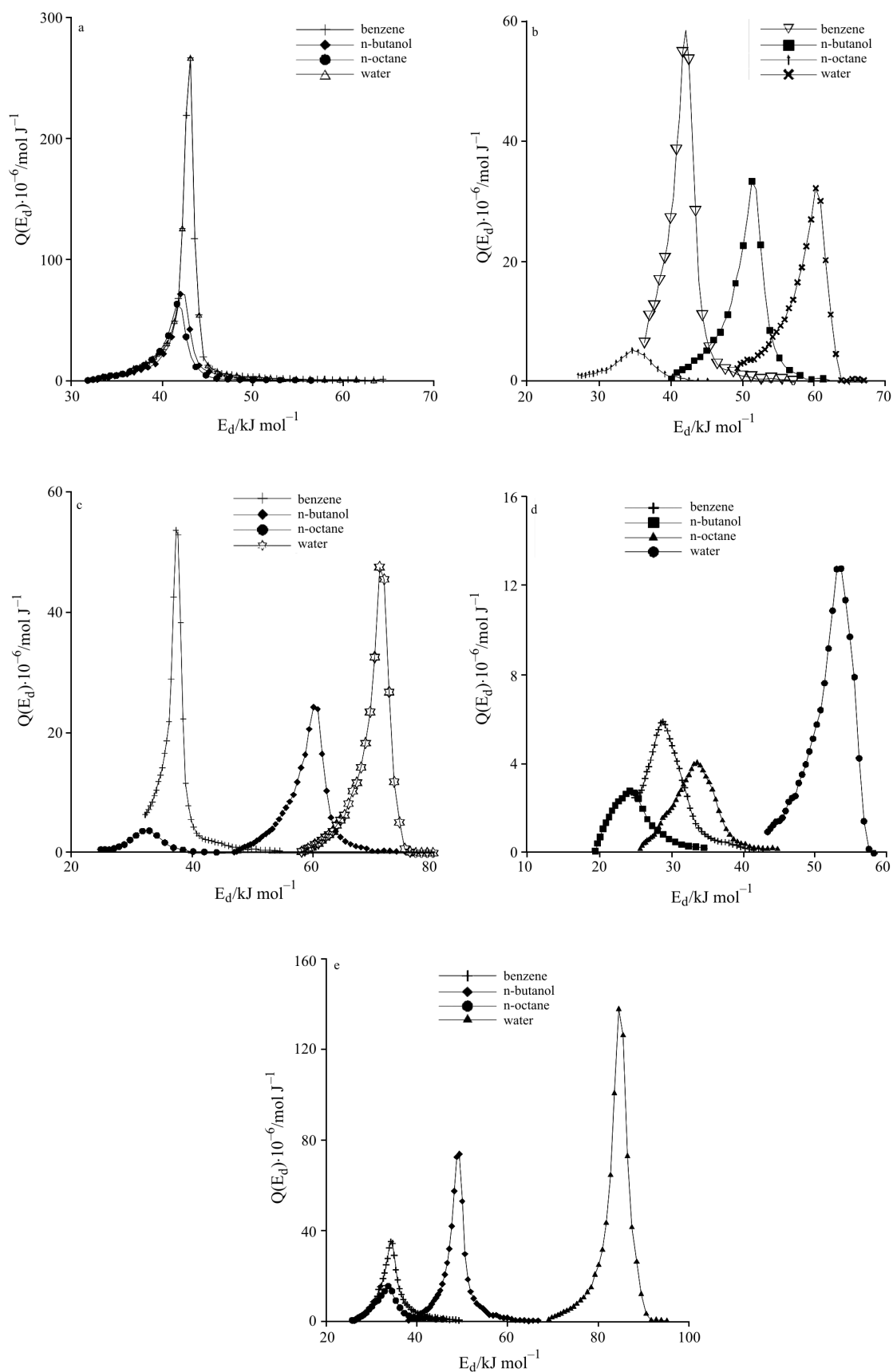


**Fig. 4** Curves of liquid desorption energy distribution functions from individual samples; a – A1, b – A2, c – A3, d – A4 and e – A5 sample

**Table 3** Comparison of *n*-butanol and water desorption energy ranges ( $\Delta E_d$  and  $E_{d,max}$  in  $\text{kJ mol}^{-1}$ ,  $Q_{E_{d,max}}$  in  $10^{-6} \text{ mol J}^{-1}$ ) for individual carbon nanotubes

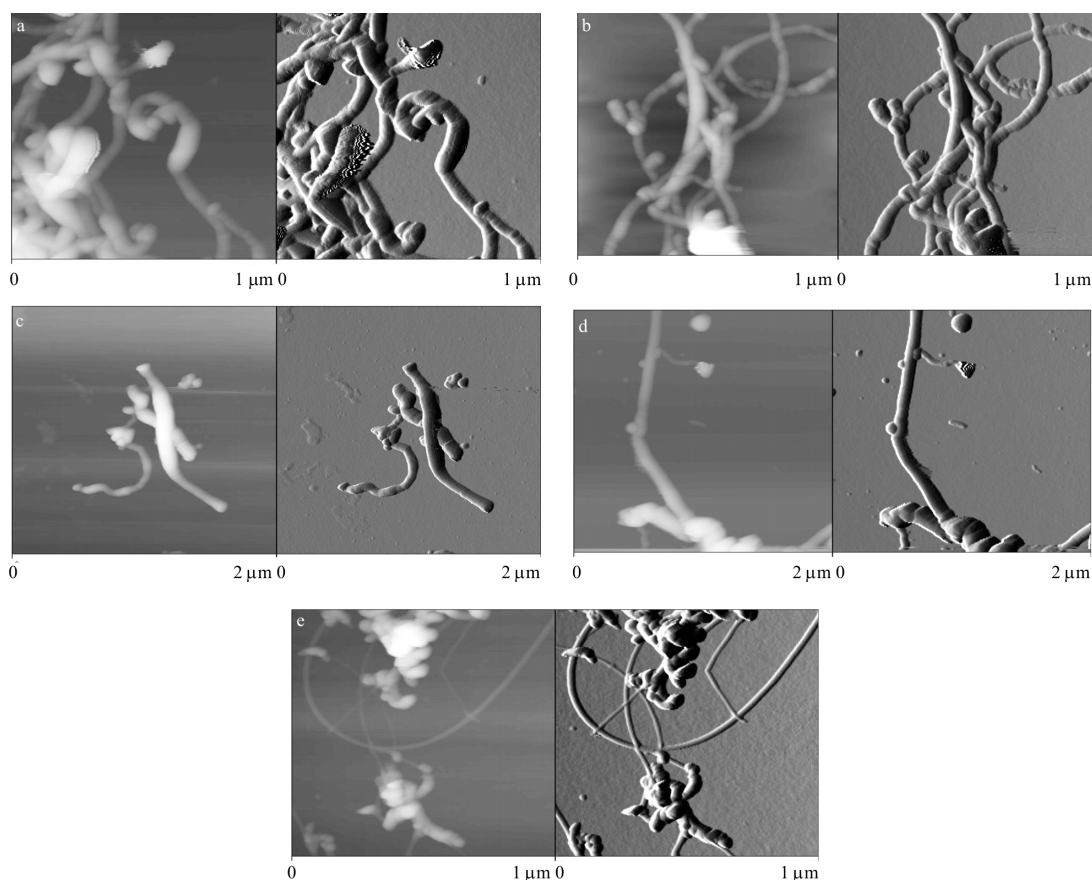
Sample	<i>n</i> -butanol			water		
	$\Delta E_d$	$E_{d,max}$	$Q_{E_{d,max}}$	$\Delta E_d$	$E_{d,max}$	$Q_{E_{d,max}}$
A1	13	42.0	51.5	6	32.3	16.5
A2	18	51.3	33.4	12	60.3	32.2
A3	20	60.1	24.2	15	71.0	47.6
A4	12	24.4	2.8	14	53.7	12.8

**Table 4** Comparison of benzene and *n*-octane desorption energy ranges ( $\Delta E_d$  and  $E_{d,max}$  in  $\text{kJ mol}^{-1}$ ,  $Q_{E_{d,max}}$  in  $10^{-6} \text{ mol J}^{-1}$ ) for individual carbon nanotubes

Sample	benzene			<i>n</i> -octane		
	$\Delta E_d$	$E_{d,max}$	$Q_{E_{d,max}}$	$\Delta E_d$	$E_{d,max}$	$Q_{E_{d,max}}$
A1	11	43.1	266.2	12	41.6	63.2
A2	15	42.1	58.5	15	34.6	5.2
A3	9	37.2	53.7	13	32.5	3.8
A4	12	28.8	5.9	15	33.6	5.1
A5	15	34.3	35.2	7	25.8	29.7

tinct peak indicating the existence of one type of main active centre on the surface of adsorbents. The  $Q_{E_d}$  value is related to the number of surface-active centres and  $E_d$  value reflects the interaction energy between ad-

sorbed molecules and sample surface. The increase of desorption energy  $E_{d,max}$  for polar liquids ( $32 < E_{d,max} < 84$  for water and  $24 < E_{d,max} < 60$  for *n*-butanol) is evidence for increase of the adsorbent–adsorbate interaction


**Fig. 5** AFM images of carbon nanotube surfaces; a – A1, b – A2, c – A3, d – A4 and e – A5

forces. Broadening of bonds on the desorption energy distribution curves indicates the increase of energetic heterogeneity of the studied materials.

#### *AFM measurements*

Figure 5 presents the images recorded by AFM microscopy. From the AFM data fractal coefficients were calculated using the commercial program in NanoScope III apparatus and are presented in Table 2.

### Conclusions

Applications of sorptometry, Q-TG thermogravimetry and AFM techniques for the investigation of adsorbed liquid layers and porosity parameters used for the quantitative characterisation of the energetic and geometrical (e.g. total) heterogeneities of carbon nanotubes are discussed. The method described is very useful to investigate physico-chemical properties of surface liquid films, adsorbate-adsorbent interactions and total nanotube surface heterogeneity. The thermodesorption process of liquids depends on the surface wetting phenomenon and surface properties of the solid surfaces.

The studies show that the thermodesorption process of liquids takes place in a continuous way as evidenced by single points of inflexion on the Q-TG curves. They are a result of interactions in the adsorbate-adsorbent system and occurrence of one main type of active centre. Studies of low-temperature ni-

trogen adsorption confirmed that the values of specific surface area ( $S_{\text{BET}}$ ) and total pore volume depend on size and structure of carbon nanotubes. Comparison of Q-TG, sorptometry and AFM data provide new information about the adsorption and structure of the studied materials.

### References

- 1 A. Huczko and P. Byszewski, Fulereny II. Charakterystyka mechanizmów powstania, PTChem., Wrocław 1998.
- 2 P. L. McEuen, Single-wall carbon nanotubes, *Physics World*, 13 (2000) 31.
- 3 G. M. Whitesides and J. C. Love, *Sztuka budowania bardzo małych struktur*. Świat Nauki., 11 (2001) 31.
- 4 P. N. Bartlett and J. J. Baumberg, *Faraday Discuss.*, 125 (2004) 118.
- 5 M. Pecul, *Nanorurki i nanotechnologia*, Młody Technik, 6 (1998) 30.
- 6 Y. C. Tovbin and E. V. Vomianov, *J. Chem. Phys.*, 67 (1993) 141.
- 7 P. Staszczuk, *J. Therm. Anal. Cal.*, 79 (2005) 545.
- 8 P. Staszczuk, M. Matyjewicz and M. Płanda, *Faculty Chem. UMCS Report*, 2002, p. 69.
- 9 P. Staszczuk, D. Sternik and V. V. Kutarov, *J. Therm. Anal. Cal.*, 69 (2002) 23.
- 10 R. C. Boetzold and G. A. Samarjai, *J. Catal.*, 45 (1976) 94.
- 11 P. Staszczuk, *J. Therm. Anal. Cal.*, 79 (2005) 545.

---

DOI: 10.1007/s10973-006-7583-5